

Hot-electron effect in spin relaxation in n -type Germanium

T. Yu and M. W. Wu*

*Hefei National Laboratory for Physical Sciences at Microscale and Department of Physics,
University of Science and Technology of China, Hefei, Anhui, 230026, China*

(Dated: February 23, 2019)

The hot-electron effect in the spin relaxation in n -type Germanium is investigated by the kinetic spin Bloch equations both analytically and numerically. It is shown that when the electric field is weak ($E \lesssim 50$ V/cm), our calculations agree fairly well with the recent transport experiment in the spin-injection configuration [Phys. Rev. Lett. **111**, 257204 (2013)]. This can explain the marked discrepancy between the experimental observation and the previous theoretical calculation [Phys. Rev. B **86**, 085202 (2012)]. We reveal that the significant enhancement of the spin relaxation at low temperature in the presence of weak electric field originates from the obvious center-of-mass drift effect due to the weak electron-phonon interaction, whereas the hot-electron effect is demonstrated to be unimportant. It is further shown that when the electric field is relatively strong with $0.5 \lesssim E \lesssim 2$ kV/cm, the spin relaxation is enhanced due to the hot-electron effect, whereas the drift effect is demonstrated to be marginal. Anomalously, we find that the impurity scattering can significantly suppress the spin relaxation in the presence of the electric field, which is a complete contrast to the Elliott-Yafet mechanism, in which the spin relaxation time is proportional to the momentum scattering. It is revealed that the contribution of the spin-flip process due to the electron-impurity scattering to the spin relaxation is marginal, and the suppression of the spin relaxation arises from the suppression of the hot-electron effect by the electron-impurity scattering. Finally, we show that when $1.4 \lesssim E \lesssim 2$ kV/cm, a small fraction of electrons ($\lesssim 5\%$) can be driven from the L to Γ valley, and the spin relaxation rates are the same for the Γ and L valleys in the impurity-free situation. With the negligible influence of the spin dynamics in the Γ valley to the whole system, the spin dynamics in the L valley can be measured from the Γ valley by the standard direct optical transition method.

PACS numbers: 75.25.Rb, 71.10.-w, 72.20.Ht, 72.10.Di

I. INTRODUCTION

Recently, growing attention has been paid to the electron spin dynamics in Germanium (Ge) due to the series of experiments including both the electrical¹⁻⁸ and optical measurements.⁹⁻¹⁴ These experimental progresses pave the way to utilize the excellent property of Ge in the spintronic application.^{3,5,12,15-22} In Ge, due to the lack of the inversion asymmetry, the D'yakov-Perel' (DP) mechanism²³ is absent. Moreover, the hyperfine interaction with the nuclei can be suppressed by the isotopic purification.^{24,25} Therefore, its spin relaxation time (SRT) is expected to be very long.^{3,5,12,15-22} Furthermore, with the mature nanoelectronic fabrication technology of the Group IV semiconductors, Ge is promising for the design and development of spintronic devices.

The electrical methods with the application of electric and/or magnetic fields include the three- or four-terminal Hanle configuration¹⁻⁷ and the spin-injection configuration.⁸ In the three- or four-terminal Hanle configuration, the typical SRTs measured are in the order of nanoseconds at low temperature and tens of picoseconds at high temperature.¹⁻⁷ In the spin-injection configuration, based on the magnetic-field-induced spin relaxation channel arising from the anisotropy of the g -factor of different L-valleys, Li *et al.* have measured the SRT by means of the spin transport under a magnetic field in the order of 100 Gauss.⁸ The SRT was measured to be

in the order of several hundreds of nanoseconds at low temperature around 50 K.⁸ Moreover, sensitive electric field dependence at weak electric fields ($\lesssim 50$ V/cm) was observed, which was speculated to be the hot-electron effect.⁸ It is noted that the SRTs measured in the spin-injection configuration are one to two orders of magnitude larger than those from the three- or four-terminal Hanle configuration. With the electrodes attached to the surface of the sample in the three- or four-terminal Hanle configuration, it was speculated that the presence of interfaces and surface roughness could have much influence on the intrinsic spin relaxation.^{2-6,26-29}

For the optical measurements, with the optical injection, several methods have been developed and applied in Ge to determine the electron SRT.⁹⁻¹⁴ Guite *et al.* have developed a novel method based on the sensitively tuned radio-frequency coil to measure the temporal evolution of the magnetization arising from the optical-injected spin polarization in Ge directly under the magnetic field (up to 80 Gauss).⁹ The temperature dependence of the electron SRT was measured to decrease from ~ 5 ns to ~ 2 ns from 100 K to 180 K.⁹ Furthermore, in the work of Lohrenz *et al.*,¹⁴ by means of the resonant spin amplification method, the electron SRT exceeding 65 ns at 60 K was measured. Moreover, a peak for the SRT appeared in the temperature dependence, which was speculated to be the influence of the electron-impurity scattering. It is noted that the SRTs measured from the optical

measurements^{9,14} are in the same order as those from the electric method in the spin-injection configuration.⁸

Meanwhile, the theoretical studies for the electron spin dynamics in Ge are in progress.^{19,21,22} With the establishment of the electron-phonon interaction in the L-valley by the group method, the SRT for the spin relaxation due to the electron-phonon scattering in the framework of the Elliott-Yafet (EY) mechanism^{30,31} has been calculated in the non-degenerate limit.^{19,21} It has been found that the main spin relaxation source in Ge comes from the inter-L valley electron-phonon interaction.^{19,21} However, up to now, there still exists marked discrepancy between the experimental observation and the theoretical calculation, especially at low temperature at which the theoretical calculations are two to three orders of magnitude larger than the experimental observations.^{7-9,14} This was speculated to be the hot-electron effect in the transport experiment⁸ or the absence of the electron-impurity scattering in the calculation.^{9,14} Therefore, a full investigation on the hot-electron effect in the spin relaxation with the inclusion of the electron-impurity scattering is needed. Moreover, although the hot-electron effect has been well studied in the charge transport experiment in Ge,^{32,33} its influence on the spin relaxation has not yet been revealed. In the charge transport experiment, it has been revealed that due to the weak electron-phonon interaction in Ge, the hot-electron effect can be easily achieved especially at low temperature.^{32,33} This feature indicates that the electric field can influence the behavior of spin relaxation easily due to the hot-electron effect.

In this work, we study the hot-electron effect in the spin relaxation in *n*-type Ge by the kinetic spin Bloch equations (KSBES)³⁴⁻³⁷ both analytically and numerically. When the electric field is weak, we compare our calculations with the recent transport experiment in the spin-injection configuration with weak electric field.⁸ Good agreements with the experimental data are obtained. It is found that due to the weak electron-phonon interaction,^{32,33} at low temperature, even small electric fields ($\lesssim 50$ V/cm)⁸ can cause obvious center-of-mass drift effect and hence significantly enhance the spin relaxation, whereas the hot-electron effect is demonstrated to be unimportant. When the electric field is relatively strong ($0.5 \lesssim E \lesssim 2$ kV/cm), we find that the SRT decreases with the increase of the electric field because of the increase of the hot-electron temperature and hence the enhancement of the electron-phonon scattering, whereas the drift effect is shown to be marginal. Anomalously, we find that the impurity scattering can suppress the spin relaxation in Ge in the presence of the electric field, which is a complete contrast to the EY mechanism, in which the SRT is proportional to the momentum scattering.^{30,31} It is revealed that the spin relaxation due to the electron-impurity scattering is marginal, and the suppression of the spin relaxation arises from the suppression of the hot-electron effect by the electron-impurity scattering and hence the electron-phonon scat-

tering. Finally, with the intra- Γ and intra-L- Γ electron-phonon interactions established by Liu *et al.*,³⁸ the influence of the Γ valley to the spin relaxation in the presence of the electric field is revealed. We find that within the strength of the electric fields we study, only a small fraction ($\lesssim 5\%$) of the electron can be driven from the L valley to the Γ valley. Therefore, the influence of the electron spin dynamics in the Γ valley to the whole system is marginal. We further reveal that in the impurity-free situation, the spin relaxation rates are the same for the Γ and L valleys, and hence the spin dynamics in the L valley can be measured from the Γ valley by the direct optical transition method.

This paper is organized as follows. In Sec. II, we set up the model and the KSBES. In Sec. III, we present the main results obtained from the KSBES both analytically and numerically. The calculated results under the weak electric field are compared with the experimental data (Sec. III A). Then, under the relatively strong electric field, the influences of the hot-electron effect on the spin relaxation are presented (Sec. III B). We summarize in Sec. IV.

II. MODEL AND KSBES

We start our investigation of the electron spin relaxation in *n*-type Ge, where the four lowest valleys in the conduction band are located at the L points [$\frac{\pi}{a_0}(1, 1, 1)$, $\frac{\pi}{a_0}(-1, 1, 1)$, $\frac{\pi}{a_0}(1, -1, 1)$ and $\frac{\pi}{a_0}(1, 1, -1)$ with a_0 denoting the lattice constant]. The Γ valley lies energetically above the L valley with $\Delta E_L^\Gamma = 0.151$ eV,³⁸ and the X valley lies further above the Γ valley with $\Delta E_\Gamma^X = 0.04$ eV.¹³ In the spherically symmetric approximation, the electron effective masses of the L and Γ valleys are $m_L^* = 0.22m_0$ ($m_l = 1.588m_0$, $m_t = 0.0815m_0$)²¹ and $m_\Gamma^* = 0.038m_0$ ($m_l = m_t = 0.038m_0$),³⁹ respectively, with m_0 representing the free electron mass. In our investigation with the electric field $E \lesssim 2$ kV/cm, we do not consider the X valley as the fraction of the electron in these valleys are negligible.

The KSBES derived via the nonequilibrium Green function method with the generalized Kadanoff-Baym Ansatz read^{34-37,40}

$$\partial_t \rho_{\lambda \mathbf{k}_\lambda} = \partial_t \rho_{\lambda \mathbf{k}_\lambda} |_{\text{drift}} + \partial_t \rho_{\lambda \mathbf{k}_\lambda} |_{\text{scat}}, \quad (1)$$

in which $\rho_{\lambda \mathbf{k}_\lambda}$ is the density matrix of electrons with momentum \mathbf{k}_λ in the λ valley. Here, \mathbf{k}_λ is defined in reference to the valley center in the valley coordinate, whose \hat{z} -axis is along the valley axis.^{21,38} The diagonal term $\rho_{\lambda \mathbf{k}_\lambda, \sigma \sigma} \equiv f_{\lambda \mathbf{k}_\lambda, \sigma}$ ($\sigma = \pm 1/2$) describes the distribution of electrons in each spin band, and the off-diagonal term $\rho_{\lambda \mathbf{k}_\lambda, \frac{1}{2} - \frac{1}{2}} = \rho_{\lambda \mathbf{k}_\lambda, -\frac{1}{2} \frac{1}{2}}^*$ represents the coherence between the two spin bands.

In the KSBES, the drift term is given by

$$\partial_t \rho_{\lambda \mathbf{k}_\lambda} |_{\text{drift}} = -e \mathbf{E} \cdot \nabla_{\lambda \mathbf{k}_\lambda} \rho_{\lambda \mathbf{k}_\lambda}, \quad (2)$$

with $e < 0$. $\partial_t \rho_{\lambda \mathbf{k}_\lambda} |_{\text{scat}}$ stands for the scattering term, which includes the electron-phonon (ep), electron-impurity (ei) and electron-electron (ee) Coulomb scatterings:

$$\partial_t \rho_{\lambda \mathbf{k}_\lambda} |_{\text{scat}} = \partial_t \rho_{\lambda \mathbf{k}_\lambda} |_{\text{ep}} + \partial_t \rho_{\lambda \mathbf{k}_\lambda} |_{\text{ei}} + \partial_t \rho_{\lambda \mathbf{k}_\lambda} |_{\text{ee}}. \quad (3)$$

Explicit forms of these scattering terms are shown in Appendix A.

The initial conditions at time $t = 0$ are prepared as follows. We turn on the electric field at $t = -t_0$, where the system is in the equilibrium, and the density matrix are expressed as

$$f_{\lambda \mathbf{k}_\lambda, \sigma}(-t_0) = \left\{ \exp[(\varepsilon_{\mathbf{k}_\lambda}^\lambda - \mu)/(k_B T)] + 1 \right\}^{-1}, \quad (4)$$

$$\rho_{\lambda \mathbf{k}_\lambda, \frac{1}{2} - \frac{1}{2}}(-t_0) = \rho_{\lambda \mathbf{k}_\lambda, -\frac{1}{2} \frac{1}{2}}^*(-t_0) = 0, \quad (5)$$

with μ being the chemical potential for the electron at temperature T . The system is driven to the steady state before $t = 0$. Then at time $t = 0$, the chemical potential is modified to obtain the spin-polarized state with the spin polarization $P_0 = (N_\uparrow - N_\downarrow)/(N_\uparrow + N_\downarrow)$. Here, $N_{\uparrow(\downarrow)} = \sum_{\lambda, \mathbf{k}_\lambda} f_{\lambda \mathbf{k}_\lambda, \uparrow(\downarrow)}$ is the electron density of spin-up (-down) state. When $t \geq 0$, the system relaxes from the spin-polarized state with the spin polarization $P(t) = \sum_{\lambda, \mathbf{k}_\lambda} \text{Tr}[\rho_{\lambda \mathbf{k}_\lambda}(t) \sigma_z]/n_e$ solved by the KSBES. Here, $n_e = \sum_{\lambda, \mathbf{k}_\lambda} \text{Tr}[\rho_{\lambda \mathbf{k}_\lambda}(t)]$ is the electron density.

III. RESULTS

A. Analytical results

Before performing the full numerical calculation by solving the KSBES, we first investigate the spin relaxation analytically with the drift effect and hot-electron effect explicitly included. It has been demonstrated that at relatively high temperature, the dominant spin relaxation channel in Ge arises from the inter-L valley electron-phonon interaction, in which the momentum dependencies of the matrix elements for the electron-phonon interaction and the phonon energy are negligible.²¹

For the electron-phonon interaction, the matrix elements can be generally constructed in this form,^{19,21,38}

$$M_{\mathbf{k}_\lambda, \mathbf{k}'_\lambda}^\gamma = A_{\mathbf{k}_\lambda, \mathbf{k}'_\lambda}^\gamma \hat{I} + \mathbf{B}_{\mathbf{k}_\lambda, \mathbf{k}'_\lambda}^\gamma \cdot \boldsymbol{\sigma}, \quad (6)$$

including both the spin-conserving and spin-flip parts for the interaction of electrons with the γ -branch phonon, where \hat{I} and $\boldsymbol{\sigma}$ are 2×2 unit and Pauli matrices. The SRT due to the inter-L valley electron-phonon interaction can be directly deduced from the scattering term [Eq. (A1)] in the KSBES ($\hbar \equiv 1$ throughout this paper)^{19,21}

$$\begin{aligned} \frac{1}{\tau_s^{\text{ep}}} &= \frac{2\pi}{Vd} \sum_{\mathbf{k}_\lambda} \sum_{\mathbf{k}'_\lambda, \lambda \neq \lambda'} \sum_{\gamma, \pm} \delta(\pm \Omega_{\mathbf{k}'_\lambda, -\mathbf{k}_\lambda}^\gamma + \varepsilon_{\mathbf{k}'_\lambda} - \varepsilon_{\mathbf{k}_\lambda}) \\ &\times \frac{1}{\Omega_{\mathbf{k}'_\lambda, -\mathbf{k}_\lambda}^\gamma} N_{\mathbf{k}'_\lambda, -\mathbf{k}_\lambda}^{\gamma, \pm} (|B_{\mathbf{k}_\lambda, \mathbf{k}'_\lambda}^{\gamma, x}|^2 + |B_{\mathbf{k}_\lambda, \mathbf{k}'_\lambda}^{\gamma, y}|^2) \\ &\times (f_{\mathbf{k}_\lambda \uparrow}^d - f_{\mathbf{k}_\lambda \downarrow}^d) \left[\sum_{\mathbf{k}_\lambda} (f_{\mathbf{k}_\lambda \uparrow}^d - f_{\mathbf{k}_\lambda \downarrow}^d) \right]^{-1}, \quad (7) \end{aligned}$$

in which, V and d are the volume and density of the crystal, respectively; γ labels the associated phonon branches in the X point connecting the two L valleys, including X_{1a} , X_{1b} , X_{4a} and X_{4b} phonons;^{19,21,38} $N_{\mathbf{k}'_\lambda, -\mathbf{k}_\lambda}^{\gamma, \pm} = N_{\mathbf{k}'_\lambda, -\mathbf{k}_\lambda}^\gamma + \frac{1}{2} \pm \frac{1}{2}$ and $N_{\mathbf{k}'_\lambda, -\mathbf{k}_\lambda}^\gamma = \left\{ \exp[\Omega_{\mathbf{k}'_\lambda, -\mathbf{k}_\lambda}^\gamma / (k_B T)] - 1 \right\}^{-1}$ is the Bose distribution of phonons with energy $\Omega_{\mathbf{k}'_\lambda, -\mathbf{k}_\lambda}^\gamma$; $f_{\mathbf{k}_\lambda \sigma}^d$ is the drifted Fermi distribution function of the electron in the steady state, which reads as^{41,42}

$$f_{\mathbf{k}_\lambda \sigma}^d = \left\{ \exp \left[\frac{(\mathbf{k}_\lambda - m_\lambda^* \mathbf{v}_\lambda)^2}{2m_\lambda^*} - \mu_\sigma \right] / (k_B T_e) + 1 \right\}^{-1}, \quad (8)$$

with \mathbf{v}_λ being the steady-state drift velocity of λ valley and T_e standing for the hot-electron temperature. In Eq. (8), \mathbf{v}_λ is numerically obtained from the steady-state value of $\mathbf{v}_\lambda(t) \equiv \sum_{\mathbf{k}_\lambda \sigma} [f_{\mathbf{k}_\lambda, \sigma}(t) \hbar \mathbf{k}_\lambda / m_\lambda] / \sum_{\mathbf{k}_\lambda \sigma} f_{\mathbf{k}_\lambda, \sigma}(t)$, and T_e is obtained by fitting the Boltzmann tail of the numerically calculated steady-state electron distribution of each valley from the KSBES.

When the electric field is weak with the condition $\frac{1}{2} m_L^* \mathbf{v}_\lambda^2 \ll k_B T_e$ or $\frac{1}{2} m_L^* \mathbf{v}_\lambda^2 \beta_e \ll 1$ [$\beta_e = 1/(k_B T_e)$] satisfied, we expand the steady-state distribution function to the order of \mathbf{v}_λ^2 . Accordingly, in the small spin polarization and non-degenerate limit, the SRT due to the inter-L valley electron-phonon interaction [Eq. (7)] can be obtained

$$\frac{1}{\tau_s^{\text{ep}}} = \sum_{\gamma} \frac{1}{\tau_s^{\text{ep}}(\mathbf{v}_\lambda = 0)} \left\{ 1 + \left[\frac{\sqrt{\pi}}{2\beta_e \Omega_\gamma} \frac{U(-0.5, -2, \beta_e \Omega_\gamma)}{K_1(\beta_e \Omega_\gamma/2)} \exp(-\beta_e \Omega_\gamma/2) - \frac{1}{2} \right] \beta_e m_L^* \mathbf{v}_\lambda^2 \right\}, \quad (9)$$

with

$$\frac{1}{\tau_s^{\text{ep}}(\mathbf{v}_\lambda = 0)} = \frac{\sqrt{\beta_e}}{8d} \left(\frac{2m_L^*}{\pi} \right)^{3/2} K_1 \left(\frac{\beta_e \Omega_\gamma}{2} \right) (|B^{\gamma, x}|^2 + |B^{\gamma, y}|^2) \frac{A_\gamma}{\sinh(\beta \Omega_\gamma/2)} \cosh \left(\frac{\beta - \beta_e}{2} \Omega_\gamma \right). \quad (10)$$

In Eqs. (9) and (10), for the inter-L valley scattering with $|\mathbf{K}_{L_i} - \mathbf{K}_{L_j}| \gg |\mathbf{k}_\lambda|$ ($i \neq j$), the momentum dependencies of the matrix elements for the electron-phonon interaction and the phonon energy are negligible,²¹ and hence their labels of momentum are omitted. $\beta = 1/(k_B T)$ with T being the lattice temperature. $A_\gamma = 16$ ($A_\gamma = 8$) for X_{1a} and X_{1b} (X_{4a} and X_{4b}) phonons.²¹ $K_1(x/2)$ and $U(-0.5, -2, x)$ are the modified Bessel function of the second kind and Tricomi's confluent hypergeometric function, respectively.

It is noted that our results in Eqs. (9) and (10) are 3/8 times of that in the work of Li *et al.* [Eq. (10) in Ref. 21] when $\beta = \beta_e$ and $\mathbf{v}_\lambda = 0$. Nevertheless, our analytical results are consistent with the numerical ones as shown in the next section (refer to Fig. 1).

From the analytical results, the effect of the drift and hot-electron effects in the spin relaxation under the weak electric field can be obtained. First of all, it can be shown that the drift effect can enhance the spin relaxation with the factor $F(x) = \frac{\sqrt{\pi}}{2x} \frac{U(-0.5, -2, x)}{K_1(x/2)} \exp(-x/2) - \frac{1}{2}$ always larger than zero. However, under the weak electric field, with $F(x)$ decreasing from 1/6 monotonically to 0 when x increases from 0, it shows that the influence of the drift effect due to the electric field to the spin relaxation is marginal when $F(x)\beta_e m_L^* \mathbf{v}_\lambda^2 \ll 1$. In this situation, the electron SRT in the presence of the electric field can be approximately obtained from Eq. (10), and hence the hot-electron effect has dominant influence on the spin relaxation. When the hot-electron temperature increases, $\sqrt{\beta_e}$ decreases slowly, $K_1(\beta_e \Omega_\gamma/2)$ increases rapidly and $\cosh[(\beta - \beta_e)\Omega_\gamma/2]$ increases slowly. Hence, the SRT decreases with the increase of the hot-electron temperature. It can also be obtained that when the lattice temperature increases, $[\sinh(\beta \Omega_\gamma/2)]^{-1}$ increases and $\cosh[(\beta - \beta_e)\Omega_\gamma/2]$ (when $\beta_e \lesssim \beta$) and $\sqrt{\beta_e}$ decrease slowly. Hence, the SRTs decreases with the increase of the lattice temperature.²¹

B. Numerical results

In this section, we present our results obtained by numerically solving the KSBEs following the scheme laid out in Refs. 43–45. All parameters including the material parameters, band structure and phonon parameters used in our computation are listed in Table I.

Before the full numerical investigation, we first divide the spin relaxation in n -type Ge in the presence of the electric field into three regimes according to the hot-electron temperature: (1) when $E \lesssim 1.4$ kV/cm, only the L valley is relevant for the spin relaxation; (2) when $1.4 \lesssim E \lesssim 2$ kV/cm, the Γ valley becomes relevant; (3) when $E \gtrsim 2$ kV/cm, the X valley becomes relevant. The boundaries between different regimes are shown in Fig. 1, where the electric field dependence of the hot-electron temperature for electrons in the L valley at different temperatures ($T = 150$ and 300 K) is presented (the

TABLE I: Parameters used in the computation.

m_L^*/m_0	0.22 ^a	Ω_{L1} (meV)	29.3 ^c
m_L^*/m_0	0.038 ^b	Ω_{L3} (meV)	7.2 ^c
ΔE_L^Γ (eV)	0.151 ^c	$\Omega_{L2'}$ (meV)	25.6 ^c
ΔE_L^X (eV)	0.04 ^d	$\Omega_{L3'}$ (meV)	35.8 ^c
$d(10^3 \text{ kg/cm}^3)$	5.323 ^e	D_{X1s} (eV/nm)	0.18 ^c
κ_0	16.0 ^f	D_{X4s} (eV/nm)	0.66 ^c
v_{LA} (m/s)	4900 ^e	D_{X1m} (eV/nm)	6.56 ^c
v_{TA} (m/s)	3500 ^e	$A_{L2'}$ (eV/nm)	18.21 ^c
$\Omega_{LO,\Gamma}$ (meV)	38.2 ^c	$B_{L3'y}$ (eV/nm)	-0.35 i^c
Ω_{X1} (meV)	28.4 ^c	P_0	30% ^d
Ω_{X4} (meV)	33.3 ^c	n_e (cm ⁻³)	5×10^{17} ^d
Ω_{X3} (meV)	10.2 ^c	t_0 (ps)	30

^aRef. 21.

^bRef. 39.

^cRef. 38.

^dRef. 13.

^eRef. 19.

^fRef. 46.

steady-state drift velocity is also shown). It can be seen that both the hot-electron temperature and the steady-state drift velocity increase with increasing the electric field. For electrons with the Boltzmann distribution and marginal drift effect ($\frac{1}{2}m_L^* \mathbf{v}_\lambda^2 \beta_e \ll 1$), its average energy is estimated to be $\bar{E} = \frac{3}{2}k_B T_e$. Accordingly, the hot-electron temperatures at which electrons can be driven to the Γ and X valleys efficiently are estimated to be $\Delta E_L^\Gamma/\bar{E} \approx 1200$ K and $(\Delta E_L^\Gamma + \Delta E_L^X)/\bar{E} \approx 1500$ K, corresponding to $E \approx 1.4$ kV/cm (shown as the black vertical dashed line) and 2 kV/cm (shown as the pink vertical dashed line) in Fig. 1, respectively. In this work, we study the spin relaxation in the presence of the electric field E up to 2 kV/cm under which the L and Γ valleys are relevant.

1. Spin relaxation under weak electric field: comparison with experiments

As mentioned in the introduction, the experiments on the electron spin relaxation in n -type Ge have been carried out recently by several methods including both the electrical^{1–8} and optical ones.^{9–14} Up to now, there still exists marked discrepancy between the experimental observations and the theoretical calculations.^{8–14,19,21,22} This motivates us to carry out the full calculations including the electron-phonon, electron-impurity and electron-electron Coulomb scatterings in the presence of the electric field. The results in the presence of the weak electric field ($E \lesssim 50$ V/cm) are summarized in Fig. 2.

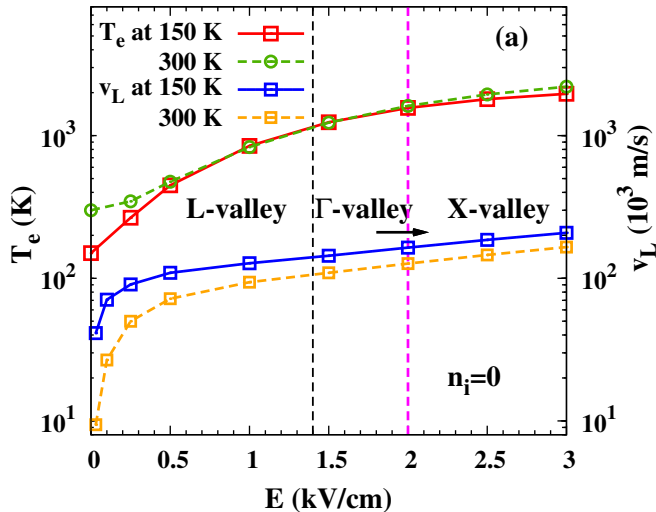


FIG. 1: (Color online) Electric field dependence of the hot-electron temperature and steady-state drift velocity (note the scale of this curve is on the right hand side of the frame) for electrons in the L valley at different temperatures (150 and 300 K). The pink (black) vertical dashed line at $E \approx 1.4$ kV/cm ($E \approx 2$ kV/cm) corresponds to the boundary at which the Γ (X) valley becomes relevant for the spin relaxation.

In Fig. 2, when electric field $E = 0$ and the electron density $n_i = n_e$, it can be seen that the SRTs with (the red solid curve with squares) and without (the blue dashed curve with circles) the electron-impurity scattering coincide with each other. Therefore, the influence of the electron-impurity scattering to the spin relaxation in the L valley is marginal. Moreover, the numerical results with all the scatterings (shown by the red solid curve with squares) are consistent with the analytical results calculated from Eq. (10) by setting $T_e = T$ (the orange dashed curve with crosses), in which only the inter-L valley scattering is included. This shows that the inter-L valley scattering is dominant for the spin relaxation.⁸ The result calculated according to Eq. (10) in Ref. 21 by Li *et al.* is also plotted by the cyan dotted curve, showing marked discrepancy compared with the full numerical result. Furthermore, it can be seen that the SRT decreases monotonically with the increase of the temperature. This is because with the increase of the temperature, the electron-phonon scattering is enhanced, which enhances the spin relaxation due to the EY mechanism.^{30,31}

When a weak electric field ($\lesssim 50$ V/cm) is applied, in Fig. 2, we compare the temperature dependence of the electron SRTs obtained from the calculations of our model with the experiments including the works of Lohrentz *et al.* (red open squares),¹⁴ Guite *et al.* (green dots),⁹ and Li *et al.* (red upward triangles for $E \approx 10$ V/cm, pink downward triangles for 30 V/cm, and blue

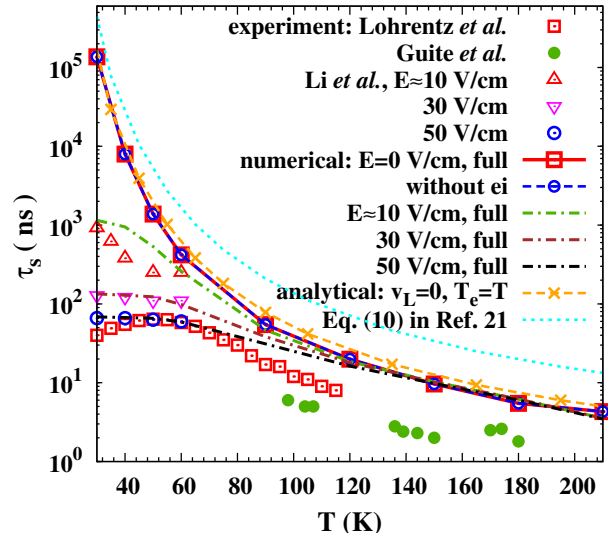


FIG. 2: (Color online) Electron SRTs in n -type Ge as function of temperature T . Experimental results: red open squares correspond to the experiment of Lohrentz *et al.* (Ref. 14); green dots represent the SRTs measured by Guite *et al.* (Ref. 9); the experimental results of Li *et al.* (Ref. 8) are shown as red upward triangles for $E \approx 10$ V/cm, pink downward triangles for $E \approx 30$ V/cm, and blue open circles for $E \approx 50$ V/cm, respectively. Numerical results: the red solid curve with squares (the blue dashed curve with circles) corresponds to the numerical result with all the scatterings (without the electron-impurity scattering) when $n_i = n_e$. The green, brown and black dot-dashed curves represent the SRTs calculated numerically with $n_i = 0.05n_e$ in the presence of the electric field $E \approx 10, 30$ and 50 V/cm, respectively. Analytical result: the orange dashed curve with crosses represents the analytical results calculated from Eq. (10) by setting $T_e = T$. The results calculated according to Eq. (10) in Ref. 21 by Li *et al.* are plotted by the cyan dotted curve.

open circles for 50 V/cm).⁸ In these experiments,^{8,9,13,14} the electrons are in the non-degenerate condition, in which the spin relaxation rates are insensitive to the electron density.^{21,34} Accordingly, without knowing the exact value of the electron density from the experiments, we choose the typical value of the electron density to be $n_e = 5 \times 10^{17} \text{ cm}^{-3}$ according to Ref. 13 (with the Fermi temperature $T_F \approx 45$ K). Moreover, in the experiment of Li *et al.*,⁸ the samples are nominally undoped, and the exact value of the impurity density is not known. In our numerical computation, we use the impurity density $n_i = 0.05n_e$ to fit the experiment (Ref. 8). It is shown that the numerical results (the green, brown and black dot-dashed curves represent the SRTs calculated numerically in the presence of the electric field $E \approx 10, 30$ and 50 V/cm, respectively) agree with the experimental observations fairly well. Moreover, we further find that with the weak electric field ($E \lesssim 50$ V/cm), the electron temperature equals to the lattice one approximately, i.e., $T_e \approx T$, whereas $\frac{1}{2}\beta_e m_L^* \mathbf{v}_L^2 \approx 2.4$ at 30 K and $\frac{1}{2}\beta_e m_L^* \mathbf{v}_L^2 \gtrsim 1$ be-

tween 40 and 60 K when $E \approx 50$ V/cm. This shows that the hot-electron effect for the system in the presence of the weak electric field at low temperature is marginal, whereas the drift effect is obvious. Therefore, this significant enhancement of the spin relaxation in the presence of the weak electric field at low temperature arises from the drift effect rather than the hot-electron effect.

One also notices that the SRTs measured by Lohrentz *et al.* (red open squares)¹⁴ and Guite *et al.* (green dots)⁹ using the optical methods lie also in the same order as those in the work of Li *et al.*,⁸ which have been understood from the drift effect induced by the weak electric field. However, these optical observations deviate from our calculations at $E=0$. It is noted that in the optical experiments, the electrons are first optically injected to the Γ valley, which are then scattered to the L and X valleys through the inter-valley electron-phonon scattering.^{9–14} Accordingly, with the weak intra-valley electron-phonon scattering,^{32,33,38} the cooling process is suppressed, and hence the hot-electron effect can arise easily.¹³ Therefore, the enhancement of the spin relaxation in the optical experiments may arise from the hot-electron effect, which has been discussed in GaAs.^{43,47,48}

2. Hot-electron effect on the spin relaxation under relatively strong electric field

In the presence of the relatively strong electric field ($0.5 \lesssim E \lesssim 2$ kV/cm), we first study the electric field dependence of the electron spin relaxation in Ge at different temperatures $T = 150$ and 400 K both numerically and analytically. In Fig. 3, the SRTs for the electrons in both the L (the red solid curves) and Γ (the blue dashed curves) valleys are plotted against the electric field, which is extended to 3 kV/cm, in the impurity-free situation.

In Fig. 3, it can be seen that for both temperatures $T = 150$ and 400 K, the SRTs in the L valley (the red solid curves) decrease monotonically with the increase of the electric field. It is noted that in Fig. 1, we have presented the electric field dependencies of the hot-electron temperature and the steady-state drift velocity, which increase with increasing electric field. From the analytical results in Sec. III A, both the drift and hot-electron effects can enhance the spin relaxation. Their contribution to the spin relaxation can be distinguished by using Eqs. (9) and (10). With the numerical values of the hot-electron temperature and the steady-state drift velocity (Fig. 1), the analytical results with (the green solid curves) and without (the black dashed curves by setting $\mathbf{v}_\lambda = 0$) the drift effect are calculated. It is shown that the two curves coincide with each other at both 150 and 400 K, which are both consistent with the numerical ones. Therefore, the influence of the drift effect to the spin relaxation at high temperature ($T \gtrsim 150$ K) is marginal. One concludes that the enhancement of the spin relaxation mainly originates from the hot-electron effect, where the increase of the hot-electron tempera-

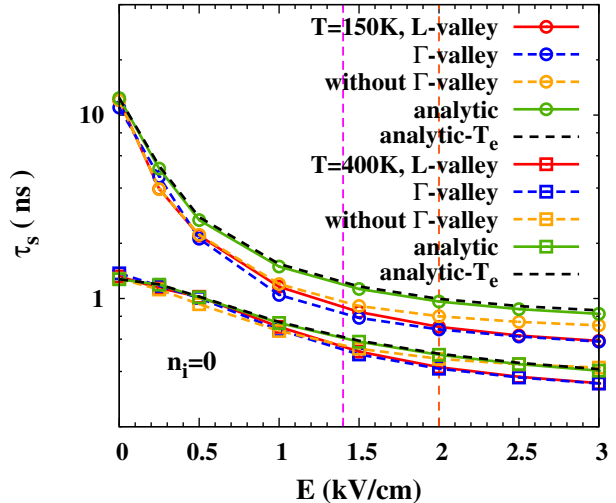


FIG. 3: (Color online) Electric field dependence of the electron SRTs in the L and Γ valleys in the impurity-free situation at 150 and 400 K, respectively. The analytical results, obtained from Eqs. (9) and (10) with the hot-electron temperature and the steady-state drift velocity numerically calculated by the KSBs, are shown by the green solid (with the drift effect) and black dashed (without the drift effect) curves.

ture enhances the electron-phonon interaction.

It has also been shown in Fig. 1 that at relatively large electric field, the Γ ($E \gtrsim 1.4$ kV/cm) and X valleys ($E \gtrsim 2$ kV/cm) become relevant. Therefore, in our study, we include the Γ valley explicitly, and reveal its influence to the spin relaxation. It is shown in Fig. 3 that at both 150 and 400 K, the SRTs in the L valley with (the red solid curves) and without (the orange dashed curves) the Γ valley are almost the same, especially at low electric field. This is because in the range of the electric field, the fractions of the electrons driven from the L to Γ valley are small ($\lesssim 5\%$), and hence the Γ valley plays a marginal role in the spin relaxation of the whole system. Moreover, the numerical results show that the SRTs in the L (the red solid curves) and Γ (the blue dashed curves) valleys are almost the same. This arises from the strong inter-L- Γ valley electron-phonon interaction and hence the frequent exchange of electrons between the L and Γ valleys.^{44,45} Accordingly, the spin dynamics in the L valley in the presence of the electric field in the impurity-free situation can be measured from the Γ valley by the standard optical method.^{49–53}

We then study the influence of the electron-impurity scattering on the spin relaxation in the presence of a relatively strong electric field $E = 1$ kV/cm at $T = 150$ K. In Fig. 4, the SRTs in the L (the blue solid curve with squares) and Γ (the blue solid curve with circles) valleys are plotted against the impurity density from 0 to $3n_e$. In Sec. III B 1, it has been shown that when the electric field is not applied, the influence of the electron-impurity

scattering on the spin relaxation is marginal. However, as shown in Fig. 4, the electron SRT in the L valley increases monotonically with the increase of the impurity density. By arbitrarily removing the spin-flip part of the electron-impurity scattering, one also observes that the SRTs in the L valley is not influenced, as shown by the orange dashed curve with crosses. By further noticing that this marked feature arises when the system is driven by the electric field, where the hot-electron effect is demonstrated to have important effect on the spin relaxation, this phenomenon can be understood from the influence of the electron-impurity scattering on the hot-electron effect.^{42,54-56} In Fig. 4, the hot-electron temperature is also plotted against the impurity density, as shown by the red solid curve with upward triangles. One finds that the hot-electron temperature decreases with the increase of the impurity density. This is understood from that when the impurity density increases, the mobility μ due to the electron-impurity scattering decreases, and hence the energy-gain rate due to the electric field $\eta = en_e\mu E^2 \propto \mu$ decreases. With the decrease of the hot-electron temperature, from Eq. (10), the spin relaxation due to the electron-phonon interaction is suppressed, leading to the increase of the SRT with the increase of the impurity density.

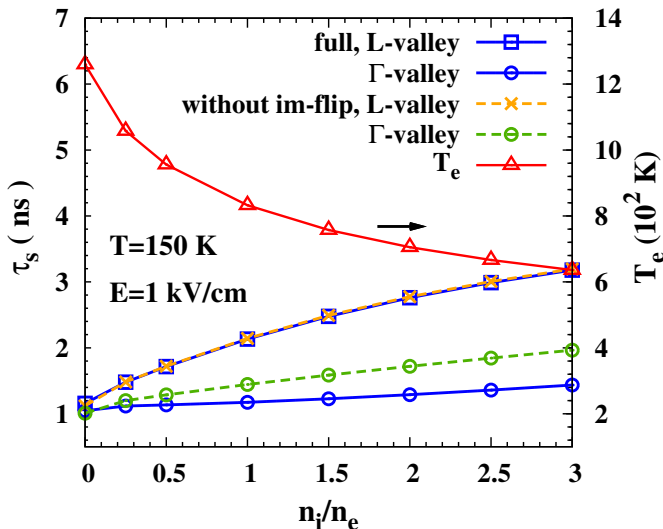


FIG. 4: (Color online) Impurity density dependence of the electron SRTs in the L and Γ valleys at $T = 150$ K in the presence of the electric field $E = 1$ kV/cm. The SRTs without the spin-flip part of the electron-impurity scattering in the L (the orange dashed curve with crosses) and Γ (the green dashed curve with circles) valleys are presented. The hot-electron temperature is shown by the red solid curve with upward triangles (note the scale of this curve is on the right hand side of the frame).

Finally, we address the new features for the spin re-

laxation behavior of the Γ valley when there exists impurities. One observes that in Fig. 4, when there exist impurities, the SRTs for Γ valleys are not the same as those in the L valley. This can be understood from the fact that when there exist impurities, the hot-electron effect is significantly suppressed, and hence the exchange of electrons between the L and Γ valleys is not efficient. Accordingly, apart from the spin dynamics in the L valley, the spin relaxation in the Γ valley is also influenced by the following three channels: the intra- Γ electron-phonon, the inter- Γ -L electron-phonon and the electron-impurity scatterings. For the intra- Γ (inter- Γ -L) electron-phonon interaction, with the spin-flip part of the matrix elements being proportional to \mathbf{k}^3 (\mathbf{k}^0),³⁸ our calculations show that the SRTs are two orders of magnitude larger than (comparable to) those due to the inter-L valley electron-phonon interaction ($\propto \mathbf{k}^0$).^{19,21,38} For the electron-impurity scattering in the Γ valley, by arbitrarily removing the spin-flip part of the electron-impurity scattering, the SRTs in the Γ valley are enhanced, as shown by the blue dashed curve with circles in Fig. 4. Therefore, very different from the situation in the L valley, the spin-flip part of the electron-impurity scattering has marked contribution to the spin relaxation in the Γ valley.

IV. SUMMARY

In summary, we have investigated the hot-electron effect in the spin relaxation in n -type Ge by the KSBES both analytically and numerically.³⁴ We first compare our calculations with the recent transport experiment by Li *et al.*⁸ in the spin-injection configuration when the electric field is weak ($\lesssim 50$ V/cm). Our calculations agree with the experimental data fairly well, and hence can explain the marked discrepancy between the experiment of Li *et al.*⁸ and the previous theoretical calculations.^{7-9,14} It is revealed that at low temperature, even small electric fields ($\lesssim 50$ V/cm)⁸ can cause obvious center-of-mass drift effect due to the weak electron-phonon interaction in Ge.^{32,33} This can significantly enhance the spin relaxation, whereas the hot-electron effect is demonstrated to be unimportant.

We then study the spin relaxation when the electric field is relatively strong ($0.5 \lesssim E \lesssim 2$ kV/cm), under which the Γ valley becomes relevant. The electric field and the impurity density dependencies of the spin relaxation are studied. In the electric field dependence, we find that the SRT decreases with the increase of the electric field. This is because with the increase of the electric field, the hot-electron temperature increases, and hence the electron-phonon scattering is enhanced. Therefore, in the presence of the relatively strong electric field, the hot-electron effect has marked influence on the spin relaxation, whereas the drift effect is shown to be marginal. In the impurity density dependence, it is unexpected to find that the impurity scattering can significantly sup-

press the spin relaxation in Ge in the presence of the electric field, which is a complete contrast to the EY mechanism, in which the SRT is proportional to the momentum scattering.^{30,31} It is revealed that the contribution of EY mechanism due to the electron-impurity scattering to the spin relaxation is marginal. We find that the suppression of the spin relaxation here arises from the suppression of the hot-electron effect by the electron-impurity scattering and hence the electron-phonon scattering.

Finally, we further study the influence of the Γ valley on the spin relaxation in the presence of the electric field. We find that within the strength of the electric fields we study ($E \lesssim 2$ kV/cm), only a small fraction ($\lesssim 5\%$) of the electron can be driven from the L valley to the Γ valley. Therefore, the influence of the electron spin dynamics in the Γ valley to the whole system is marginal. Nevertheless, we find that in the impurity-free situation, the spin relaxation rates are the same for the Γ and L valleys, and hence the spin dynamics in the L valley can be measured from the Γ valley by the standard optical methods.

Acknowledgments

This work was supported by the National Natural Science Foundation of China under Grant No. 11334014, the National Basic Research Program of China under

Grant No. 2012CB922002 and the Strategic Priority Research Program of the Chinese Academy of Sciences under Grant No. XDB01000000. One of the authors (TY) would like to thank M. Q. Weng for suggestion on analytical derivation.

Appendix A: Scattering terms of the KSBEs

The scattering terms for the electron-phonon, electron-impurity and electron-electron scatterings are shown as,

$$\begin{aligned} \partial_t \rho_{\lambda \mathbf{k}_\lambda} |_{\text{ep}} = & -\pi \sum_{\lambda', \mathbf{k}'_\lambda, \pm} \sum_{\gamma} \delta(\pm \Omega_{\mathbf{k}'_\lambda, -\mathbf{k}_\lambda}^\gamma + \varepsilon_{\mathbf{k}'_\lambda}^{\lambda'} - \varepsilon_{\mathbf{k}_\lambda}^\lambda) \\ & \times \left(N_{\mathbf{k}'_\lambda, -\mathbf{k}_\lambda}^{\gamma, \pm} M_{\mathbf{k}_\lambda, \mathbf{k}'_\lambda}^\gamma \rho_{\lambda' \mathbf{k}'_\lambda}^\gamma M_{\mathbf{k}'_\lambda, \mathbf{k}_\lambda}^\gamma \rho_{\lambda \mathbf{k}_\lambda}^\gamma - N_{\mathbf{k}'_\lambda, -\mathbf{k}_\lambda}^{\gamma, \mp} \right. \\ & \left. \times M_{\mathbf{k}_\lambda, \mathbf{k}'_\lambda}^\gamma \rho_{\lambda' \mathbf{k}'_\lambda}^\gamma M_{\mathbf{k}'_\lambda, \mathbf{k}_\lambda}^\gamma \rho_{\lambda \mathbf{k}_\lambda}^\gamma \right) + \text{H.c.}; \end{aligned} \quad (\text{A1})$$

$$\begin{aligned} \partial_t \rho_{\lambda \mathbf{k}_\lambda} |_{\text{ei}} = & -\pi n_i Z_i^2 \sum_{\mathbf{k}'_\lambda} V_{\mathbf{k}_\lambda - \mathbf{k}'_\lambda}^2 \left(\hat{\Lambda}_{\lambda \mathbf{k}_\lambda, \lambda \mathbf{k}'_\lambda} \rho_{\lambda' \mathbf{k}'_\lambda}^\gamma \hat{\Lambda}_{\lambda \mathbf{k}'_\lambda, \lambda \mathbf{k}_\lambda} \rho_{\lambda \mathbf{k}_\lambda}^\gamma \right. \\ & \left. - \hat{\Lambda}_{\lambda \mathbf{k}_\lambda, \lambda \mathbf{k}'_\lambda} \rho_{\lambda' \mathbf{k}'_\lambda}^\gamma \hat{\Lambda}_{\lambda \mathbf{k}'_\lambda, \lambda \mathbf{k}_\lambda} \rho_{\lambda \mathbf{k}_\lambda}^\gamma \right) \delta(\varepsilon_{\mathbf{k}'_\lambda}^{\lambda'} - \varepsilon_{\mathbf{k}_\lambda}^\lambda) + \text{H.c.}; \end{aligned} \quad (\text{A2})$$

$$\begin{aligned} \partial_t \rho_{\lambda \mathbf{k}_\lambda} |_{\text{ee}} = & -\pi \sum_{\lambda', \mathbf{k}'_\lambda, \mathbf{k}''_\lambda} V_{\mathbf{k}_\lambda - \mathbf{k}'_\lambda}^2 \delta(\varepsilon_{\mathbf{k}'_\lambda}^\lambda - \varepsilon_{\mathbf{k}_\lambda}^\lambda + \varepsilon_{\mathbf{k}''_\lambda}^{\lambda'} - \varepsilon_{\mathbf{k}'_\lambda, -\mathbf{k}_\lambda + \mathbf{k}'_\lambda}^{\lambda'}) \\ & \times \left\{ \hat{\Lambda}_{\lambda \mathbf{k}_\lambda, \lambda \mathbf{k}'_\lambda} \rho_{\lambda' \mathbf{k}'_\lambda}^\gamma \hat{\Lambda}_{\lambda \mathbf{k}'_\lambda, \lambda \mathbf{k}_\lambda} \rho_{\lambda \mathbf{k}_\lambda}^\gamma \text{Tr} \left[\hat{\Lambda}_{\lambda' \mathbf{k}''_\lambda, \lambda' (\mathbf{k}'_\lambda, -\mathbf{k}_\lambda + \mathbf{k}'_\lambda)} \rho_{\lambda' (\mathbf{k}'_\lambda, -\mathbf{k}_\lambda + \mathbf{k}'_\lambda)}^\gamma \hat{\Lambda}_{\lambda' (\mathbf{k}'_\lambda, -\mathbf{k}_\lambda + \mathbf{k}'_\lambda), \lambda' \mathbf{k}''_\lambda} \rho_{\lambda' \mathbf{k}''_\lambda}^\gamma \right] \right. \\ & \left. - \hat{\Lambda}_{\lambda \mathbf{k}_\lambda, \lambda \mathbf{k}'_\lambda} \rho_{\lambda' \mathbf{k}'_\lambda}^\gamma \hat{\Lambda}_{\lambda \mathbf{k}'_\lambda, \lambda \mathbf{k}_\lambda} \rho_{\lambda \mathbf{k}_\lambda}^\gamma \text{Tr} \left[\hat{\Lambda}_{\lambda' \mathbf{k}''_\lambda, \lambda' (\mathbf{k}'_\lambda, -\mathbf{k}_\lambda + \mathbf{k}'_\lambda)} \rho_{\lambda' (\mathbf{k}'_\lambda, -\mathbf{k}_\lambda + \mathbf{k}'_\lambda)}^\gamma \hat{\Lambda}_{\lambda' (\mathbf{k}'_\lambda, -\mathbf{k}_\lambda + \mathbf{k}'_\lambda), \lambda' \mathbf{k}''_\lambda} \rho_{\lambda' \mathbf{k}''_\lambda}^\gamma \right] \right\} + \text{H.c.} \quad (\text{A3}) \end{aligned}$$

Here, $\rho_{\mathbf{k}}^\leftarrow = \rho_{\mathbf{k}}$ and $\rho_{\mathbf{k}}^\rightarrow = 1 - \rho_{\mathbf{k}}$. $\varepsilon_{\mathbf{k}_{L_i}}^{L_i} = k_{L_i}^2 / (2m_L^*)$ and $\varepsilon_{\mathbf{k}_\Gamma}^\Gamma = k_\Gamma^2 / (2m_\Gamma^*) + \Delta E_\Gamma^\Gamma$. In Eq. (A1), for the intra- Γ valley electron-phonon scattering ($\lambda = \lambda' = \Gamma$), the phonon branches include TA₁, TA₂, LA, TO₁, TO₂, and LO phonons, where the electron-phonon scattering with the \mathbf{k}^0 -order is forbidden [for the spin-conserving (spin-flip) scattering, the matrix elements are proportional to \mathbf{k} (\mathbf{k}^3)].³⁸ For the intra-L valley scattering ($\lambda = \lambda' = \text{L}$), the phonon branches include TO₁, TO₂, and LO phonons, and especially for the spin-flip scattering, the matrix elements are proportional to \mathbf{k}^3 , which are neglected in our study when the inter-L valley scattering is dominant for spin relaxation.^{21,38} For the inter- Γ -L valley scattering, the phonon branches include L₁, L₃, L_{2'}, and L_{3'} phonons, where the electron-phonon interactions with \mathbf{k}^0 -order exist for both the spin-conserving

and spin-flip scatterings.³⁸ For the inter-L valley electron-phonon scattering, the phonon branches include X₁ and X₄ phonons, where the electron-phonon interactions with \mathbf{k}^0 -order also exist for both the spin-conserving and spin-flip scatterings,^{21,38} and especially we add the electron-phonon scattering with the \mathbf{k} -order.³⁸

In Eqs. (A2) and (A3), n_i is the impurity density and $Z_i = 1$ is the charge number of the impurity; $V_{\mathbf{q}}$ is the screened Coulomb potential under the random phase approximation.^{34,43-45} The spin mixing $\hat{\Lambda}_{\lambda \mathbf{k}_\lambda, \lambda' \mathbf{k}'_\lambda} = \hat{I} - \frac{1}{2} [S_{\lambda \mathbf{k}_\lambda}^{(1)} S_{\lambda \mathbf{k}_\lambda}^{(1)\dagger} - 2S_{\lambda \mathbf{k}_\lambda}^{(1)} S_{\lambda' \mathbf{k}'_\lambda}^{(1)\dagger} + S_{\lambda' \mathbf{k}'_\lambda}^{(1)} S_{\lambda' \mathbf{k}'_\lambda}^{(1)\dagger}]$. The matrix $S_{\lambda' \mathbf{k}'_\lambda}^{(1)}$ for the Γ and L valleys can be found in the 14×14 $\mathbf{k} \cdot \mathbf{p}$ Hamiltonian³⁹ and 16×16 one,³⁸ whose explicit forms are shown as follows. For the Γ valley,

$$S_{\Gamma_{\mathbf{k}r}}^{(1)} = \begin{pmatrix} \frac{1}{\sqrt{2}} \frac{P^+}{E_g} & -\sqrt{\frac{2}{3}} \frac{P^z}{E_g} & -\frac{1}{\sqrt{6}} \frac{P^-}{E_g} & 0 & -\frac{1}{\sqrt{3}} \frac{P^z}{E_g + \Delta} & -\frac{1}{\sqrt{3}} \frac{P^-}{E_g + \Delta} \\ 0 & \frac{1}{\sqrt{6}} \frac{P^+}{E_g} & -\sqrt{\frac{2}{3}} \frac{P^z}{E_g} & -\frac{1}{\sqrt{2}} \frac{P^-}{E_g} & -\frac{1}{\sqrt{3}} \frac{P^+}{E_g + \Delta} & \frac{1}{\sqrt{3}} \frac{P^z}{E_g + \Delta} \end{pmatrix}, \quad (\text{A4})$$

where $P^z = Pk_z$, $P^\pm = Pk_\pm = P(k_x \pm k_y)$ with $E_P = (2/m_0)P^2 = 26.3$ eV, $E_g = 0.898$ eV and $\Delta = 0.297$ eV.³⁹ For the L valley,

$$S_{L\mathbf{k}_L}^{(1)} = \left(S_{L\mathbf{k}_L}^{\text{left}}, S_{L\mathbf{k}_L}^{\text{right}} \right), \quad (\text{A5})$$

where

$$S_{L\mathbf{k}_L}^{\text{left}} = \begin{pmatrix} \frac{\alpha_4 k_-}{E_{c1} - E_{c6}} & -\frac{P_4 k_z}{E_{c1} - E_{c6}} & \frac{\sqrt{2}(P_3 - \alpha_3)k_-}{E_{c1} - E_{c5}} & \frac{2\sqrt{2}\alpha_3 k_z}{E_{c1} - E_{c5}} & -\frac{(P_3 + \alpha_3)k_+}{E_{c1} - E_{c4}} & \frac{(P_3 + \alpha_3)k_+}{E_{c1} - E_{c4}} \\ -\frac{P_4 k_z}{E_{c1} - E_{c6}} & -\frac{\alpha_4 k_+}{E_{c1} - E_{c6}} & \frac{2\sqrt{2}\alpha_3 k_z}{E_{c1} - E_{c5}} & \frac{\sqrt{2}(\alpha_3 - P_3)k_+}{E_{c1} - E_{c5}} & -\frac{(P_3 + \alpha_3)k_-}{E_{c1} - E_{c4}} & -\frac{(P_3 + \alpha_3)k_-}{E_{c1} - E_{c4}} \end{pmatrix}, \quad (\text{A6})$$

and

$$S_{L\mathbf{k}_L}^{\text{right}} = \begin{pmatrix} -\frac{\Delta_2}{E_{c1} - E_{c2}} & 0 & -\frac{(P_1 + \alpha_1)k_+}{E_{c1} - E_{v1}} & \frac{(P_1 + \alpha_1)k_+}{E_{c1} - E_{v1}} & -\frac{2\sqrt{2}\alpha_1 k_z}{E_{c1} - E_{v2}} & \frac{\sqrt{2}(2\alpha_1 - P_1)k_-}{E_{c1} - E_{v2}} \\ 0 & -\frac{\Delta_2}{E_{c1} - E_{c2}} & \frac{(P_1 + \alpha_1)k_-}{E_{c1} - E_{v1}} & \frac{(P_1 + \alpha_1)k_-}{E_{c1} - E_{v1}} & \frac{\sqrt{2}(P_1 - 2\alpha_1)k_+}{E_{c1} - E_{v2}} & -\frac{2\sqrt{2}\alpha_1 k_z}{E_{c1} - E_{v2}} \end{pmatrix}. \quad (\text{A7})$$

All the parameters in Eqs. (A6) and (A7) are listed in Table I of Ref. 38.

* Author to whom correspondence should be addressed; Electronic address: mwwu@ustc.edu.cn.

¹ C. Shen, T. Trypiniotis, K. Y. Lee, S. N. Holmes, R. Mansell, M. Husain, V. Shah, X. V. Li, H. Kurebayashi, I. Farrer, C. H. de Groot, D. R. Leadley, G. Bell, E. H. C. Parker, T. Whall, D. A. Ritchie, and C. H. W. Barnes, *Appl. Phys. Lett.* **97**, 162104 (2010).

² H. Saito, S. Watanabe, Y. Mineno, S. Sharma, R. Jansen, S. Yuasa, and K. Ando, *Solid State Commun.* **151**, 1159 (2011).

³ Y. Zhou, W. Han, L. T. Chang, F. Xiu, M. Wang, M. Oehme, I. A. Fischer, J. Schulze, R. K. Kawakami, and K. L. Wang, *Phys. Rev. B* **84**, 125323 (2011).

⁴ K. R. Jeon, B. C. Min, Y. H. Jo, H. S. Lee, I. J. Shin, C. Y. Park, S. Y. Park, and S. C. Shin, *Phys. Rev. B* **84**, 165315 (2011).

⁵ A. Jain, L. Louahadj, J. Peiro, J. C. Le Breton, C. Vergnaud, A. Barski, C. Beigné, L. Notin, A. Marty, V. Baltz, S. Auffret, E. Augendre, H. Jaffrés, J. M. George, and M. Jamet, *Appl. Phys. Lett.* **99**, 162102 (2011).

⁶ K. Kasahara, Y. Baba, K. Yamane, Y. Ando, S. Yamada, Y. Hoshi, K. Sawano, M. Miyao and K. Hamaya, *J. Appl. Phys.* **111**, 07C503 (2012).

⁷ L. T. Chang, W. Han, Y. Zhou, J. Tang, I. A. Fischer,

M. Oehme, J. Schulze, R. K. Kawakami and K. L. Wang, *Semicond. Sci. Technol.* **28** 015018 (2013).

⁸ P. Li, J. Li, L. Qing, H. Dery, and I. Appelbaum, *Phys. Rev. Lett.* **111**, 257204 (2013).

⁹ C. Guite and V. Venkataraman, *Phys. Rev. Lett.* **107**, 166603 (2011); *Appl. Phys. Lett.* **101**, 252404 (2012).

¹⁰ C. Hautmann, B. Surrer, and M. Betz, *Phys. Rev. B* **83**, 161203 (R) (2011).

¹¹ C. Hautmann and M. Betz, *Phys. Rev. B* **85**, 121203 (R) (2012).

¹² F. Pezzoli, F. Bottegioni, D. Trivedi, F. Ciccacci, A. Giorgioni, P. Li, S. Cecchi, E. Grilli, Y. Song, M. Guzzi, H. Dery, and G. Isella, *Phys. Rev. Lett.* **108**, 156603 (2012).

¹³ F. Pezzoli, L. Qing, A. Giorgioni, G. Isella, E. Grilli, M. Guzzi, and H. Dery, *Phys. Rev. B* **88**, 045204 (2013).

¹⁴ J. Lohrenz, T. Paschen, and M. Betz, *Phys. Rev. B* **89**, 121201 (R) (2014).

¹⁵ E. J. Loren, B. A. Ruzicka, L. K. Werake, H. Zhao, H. M. van Driel, and A. L. Smirl, *Appl. Phys. Lett.* **95**, 092107 (2009).

¹⁶ J. Rioux and J. E. Sipe, *Phys. Rev. B* **81**, 155215 (2010).

¹⁷ E. J. Loren, J. Rioux, C. Lange, J. E. Sipe, H. M. van Driel, and A. L. Smirl, *Phys. Rev. B* **84**, 214307 (2011).

¹⁸ P. Li and H. Dery, *Phys. Rev. Lett.* **107**, 107203 (2011).

- ¹⁹ J. M. Tang, B. T. Collins, and M. E. Flatté, *Phys. Rev. B* **85**, 045202 (2012).
- ²⁰ A. Jain, C. Vergnaud, J. Peiro, J. C. Le Breton, E. Prestat, L. Louahadj, C. Portemont, C. Ducruet, V. Baltz, A. Marty, A. Barski, P. B. Guillemaud, L. Vila, J. P. Attané, E. Augendre, H. Jaffrès, J. M. George, and M. Jamet, *Appl. Phys. Lett.* **101**, 022402 (2012).
- ²¹ P. Li, Y. Song, and H. Dery, *Phys. Rev. B* **86**, 085202 (2012).
- ²² P. Li, D. Trivedi, and H. Dery, *Phys. Rev. B* **87**, 115203 (2013).
- ²³ M. I. D'yakonov and V. I. Perel', *Zh. Eksp. Teor. Fiz.* **60**, 1954 (1971) [*Sov. Phys. JETP* **33**, 1053 (1971)].
- ²⁴ B. E. Kane, *Nature (London)* **393**, 133 (1998).
- ²⁵ P. S. Fodor and J. Levy, *J. Phys.: Condens. Matter* **18**, S745 (2006).
- ²⁶ M. Tran, H. Jaffrès, C. Deranlot, J. M. George, A. Fert, A. Miard, and A. Lemaître, *Phys. Rev. Lett.* **102**, 036601 (2009).
- ²⁷ S. P. Dash, S. Sharma, J. C. Le Breton, J. Peiro, H. Jaffrès, J. M. George, A. Lemaître, and R. Jansen, *Phys. Rev. B* **84**, 054410 (2011).
- ²⁸ C. H. Li, O. M. J. van't Erve, and B. T. Jonker, *Nature Commun.* **2**, 245 (2011).
- ²⁹ S. P. Dash, S. Sharma, R. S. Patel, M. P. de Jong, and R. Jansen, *Nature (London)* **462**, 491 (2009).
- ³⁰ Y. Yafet, *Phys. Rev.* **85**, 478 (1952).
- ³¹ R. J. Elliott, *Phys. Rev.* **96**, 266 (1954).
- ³² J. C. McGroddy, M. I. Nathan, and J. E. Smith, Jr *IBM J. Res. DeV.* **13**, 543 (1969).
- ³³ C. Jacoboni, F. Nava, C. Canali, and G. Ottaviani, *Phys. Rev. B* **24**, 1014 (1981).
- ³⁴ M. W. Wu, J. H. Jiang, and M. Q. Weng, *Phys. Rep.* **493**, 61 (2010).
- ³⁵ M. W. Wu and H. Metiu, *Phys. Rev. B* **61**, 2945 (2000).
- ³⁶ M. W. Wu and C. Z. Ning, *Eur. Phys. J. B.* **18**, 373 (2000); M. W. Wu, *J. Phys. Soc. Jpn.* **70**, 2195 (2001).
- ³⁷ M. Q. Weng and M. W. Wu, *Phys. Rev. B* **68**, 075312 (2003).
- ³⁸ Z. Liu, M. O. Nestoklon, J. L. Cheng, E. L. Ivchenko, and M. W. Wu, *Fizika Tverdogo Tela* **55**, 1510 (2013) [*Phys. Solid State* **55**, 1619 (2013)].
- ³⁹ S. Ridene, K. Boujdaria, H. Bouchriha, and G. Fishman, *Phys. Rev. B* **64**, 085329 (2001).
- ⁴⁰ H. Haug and A. P. Jauho, *Quantum Kinetics in Transport and Optics of Semiconductors* (Springer, Berlin, 1996).
- ⁴¹ E. M. Lifshitz and L. P. Pitaevskii, *Physical Kinetics* (Pergamon, London, 1981); G. E. Uhlenbeck, G. W. Ford, and E. W. Montroll, *Lectures in Statistical Mechanics* (American Mathematical Society, Providence, 1963), Chap. IV; V. F. Gantmakher and Y. B. Levinson, *Carrier Scattering in Metals and Semiconductors* (North-Holland, Amsterdam, 1987), Chap. 6.
- ⁴² X. L. Lei, *Balance Equation Approach to Electron Transport in Semiconductors* (World Scientific, Singapore, 2008).
- ⁴³ J. H. Jiang and M. W. Wu, *Phys. Rev. B* **79**, 125206 (2009); **83**, 239906(E) (2011).
- ⁴⁴ P. Zhang, J. Zhou, and M. W. Wu, *Phys. Rev. B* **77**, 235323 (2008).
- ⁴⁵ H. Tong and M. W. Wu, *Phys. Rev. B* **85**, 075203 (2012).
- ⁴⁶ *Numerical Data and Functional Relationships in Science and Technology*, Landolt-Börnstein, New Series, Group III, Vol. 17, Pt. A, edited by O. Madelung, M. Schultz, and H. Weiss (Springer-Verlag, Berlin, 1982).
- ⁴⁷ K. Shen, *Chin. Phys. Lett.* **26**, 067201 (2009).
- ⁴⁸ M. Krauß, H. C. Schneider, R. Bratschitsch, Z. Chen, and S. T. Cundiff, *Phys. Rev. B* **81**, 035213 (2010).
- ⁴⁹ N. Tombros, S. Tanabe, A. Veligura, C. Józsa, M. Popinciuc, H. T. Jonkman, and B. J. van Wees, *Phys. Rev. Lett.* **101**, 046601 (2008).
- ⁵⁰ *Semiconductor Spintronics and Quantum Computation*, edited by D. D. Awschalom, D. Loss, and N. Samarth (Springer, Berlin, 2002).
- ⁵¹ J. A. Gupta, R. Knobel, N. Samarth, and D. D. Awschalom, *Science* **292**, 2458 (2001).
- ⁵² S. A. Wolf, D. D. Awschalom, R. A. Buhrman, J. M. Daughton, S. von Molnár, M. L. Roukes, A. Y. Chtchelkanova, and D. M. Treger, *Science* **294**, 1488 (2001).
- ⁵³ T. Korn, *Phys. Rep.* **494**, 415 (2010).
- ⁵⁴ E. M. Conwell, *High Field Transport in Semiconductors* (Academic Press, New York, 1967).
- ⁵⁵ X. L. Lei and C. S. Ting, *Phys. Rev. B* **30**, 4809 (1984).
- ⁵⁶ K. Seeger, *Semiconductor Physics: An Introduction* (Springer, 2004).